

# **The impact of mutational clonality in predicting the response to immune checkpoint inhibitors in advanced urothelial cancer**

Lilian Marie Boll<sup>1\*</sup>, Júlia Perera-Bel<sup>1\*</sup>, Alejo Rodriguez-Vida<sup>1,2,3</sup>, Oriol Arpí<sup>1</sup>, Ana Rovira<sup>1,2,3</sup>, Núria Juanpere Roderó<sup>1</sup>, Sergio Vázquez Montes de Oca<sup>1</sup>, Silvia Hernández-Llodrà<sup>4</sup>, Josep Lloreta<sup>1,4</sup>, M. Mar Albà<sup>1,5,#</sup>, Joaquim Bellmunt<sup>1,6,#</sup>

<sup>1</sup>PSMAR-IMIM Research Institute, Barcelona, Spain.

<sup>2</sup>Medical Oncology Department, Hospital del Mar, Barcelona, Spain.

<sup>3</sup>Centro de Investigación Biomédica en Red de Oncología (CIBERONC-ISCIII), Barcelona, Spain.

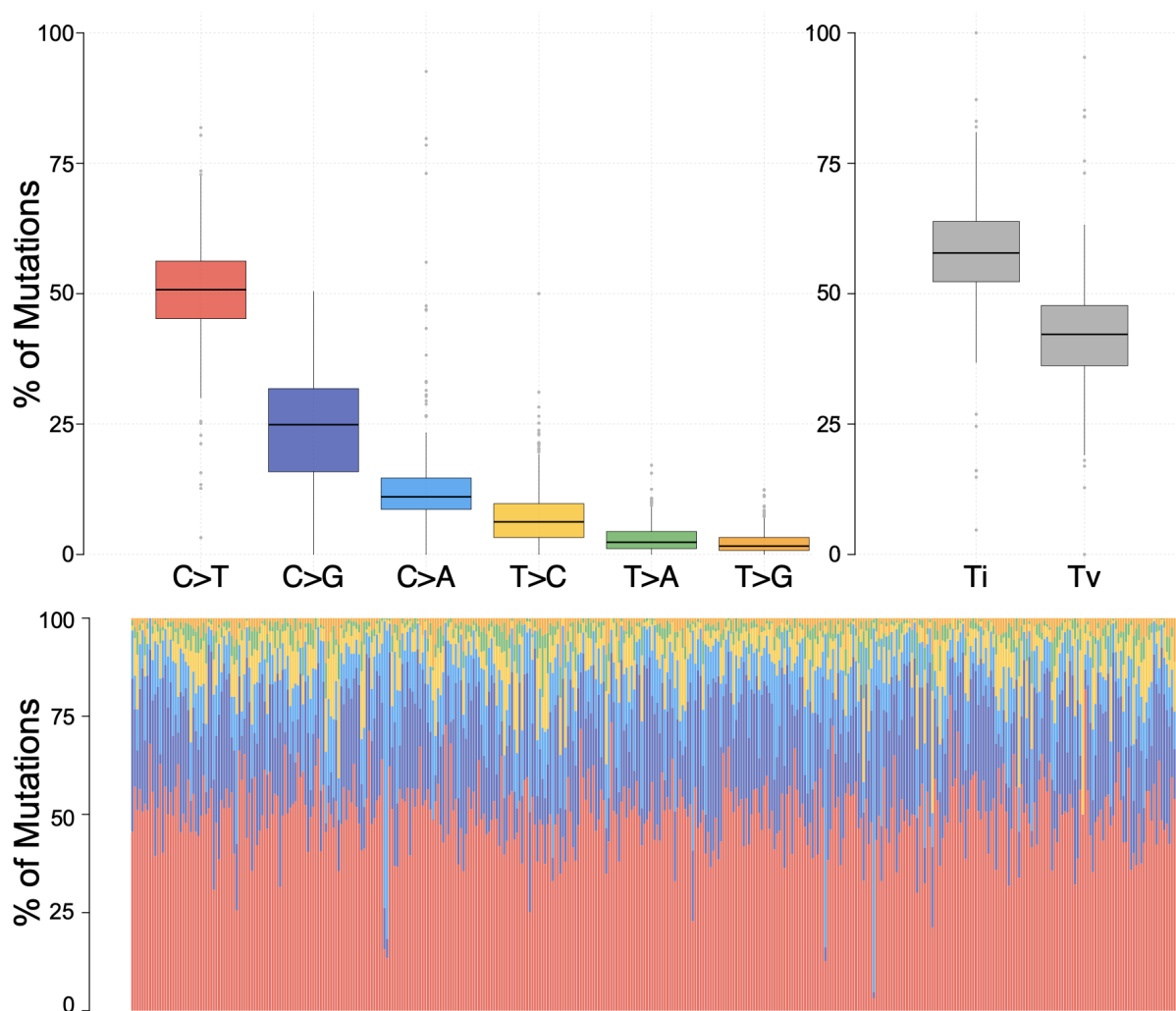
<sup>4</sup>Department of Medicine and Life Science, Universitat Pompeu Fabra (UPF), Barcelona, Spain.

<sup>5</sup>Catalan Institute for Research and Advanced Studies (ICREA).

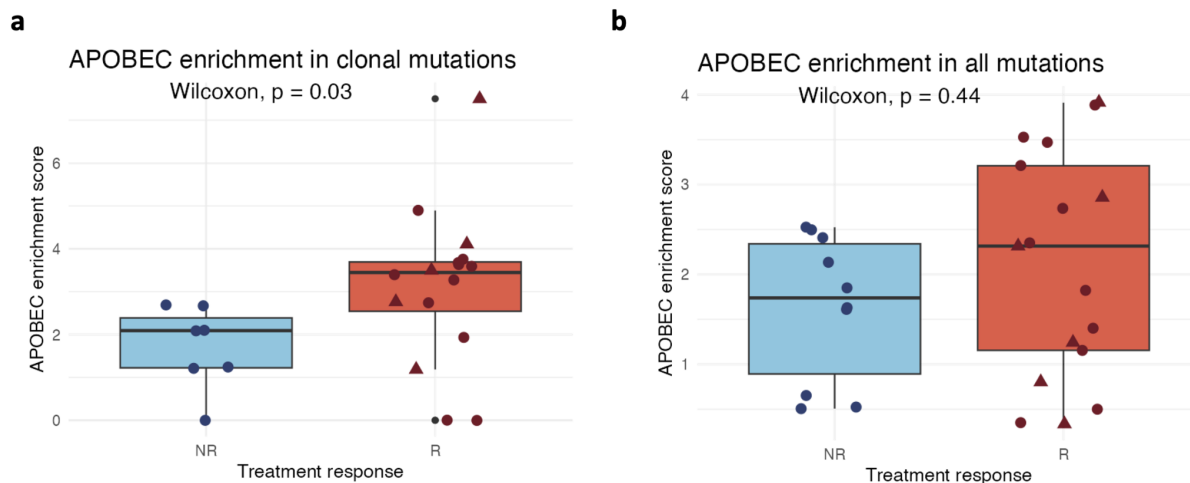
<sup>6</sup>Dana Farber Cancer Institute & IMIM Research Lab., Harvard Medical School Boston Massachusetts.

\*co-first authors

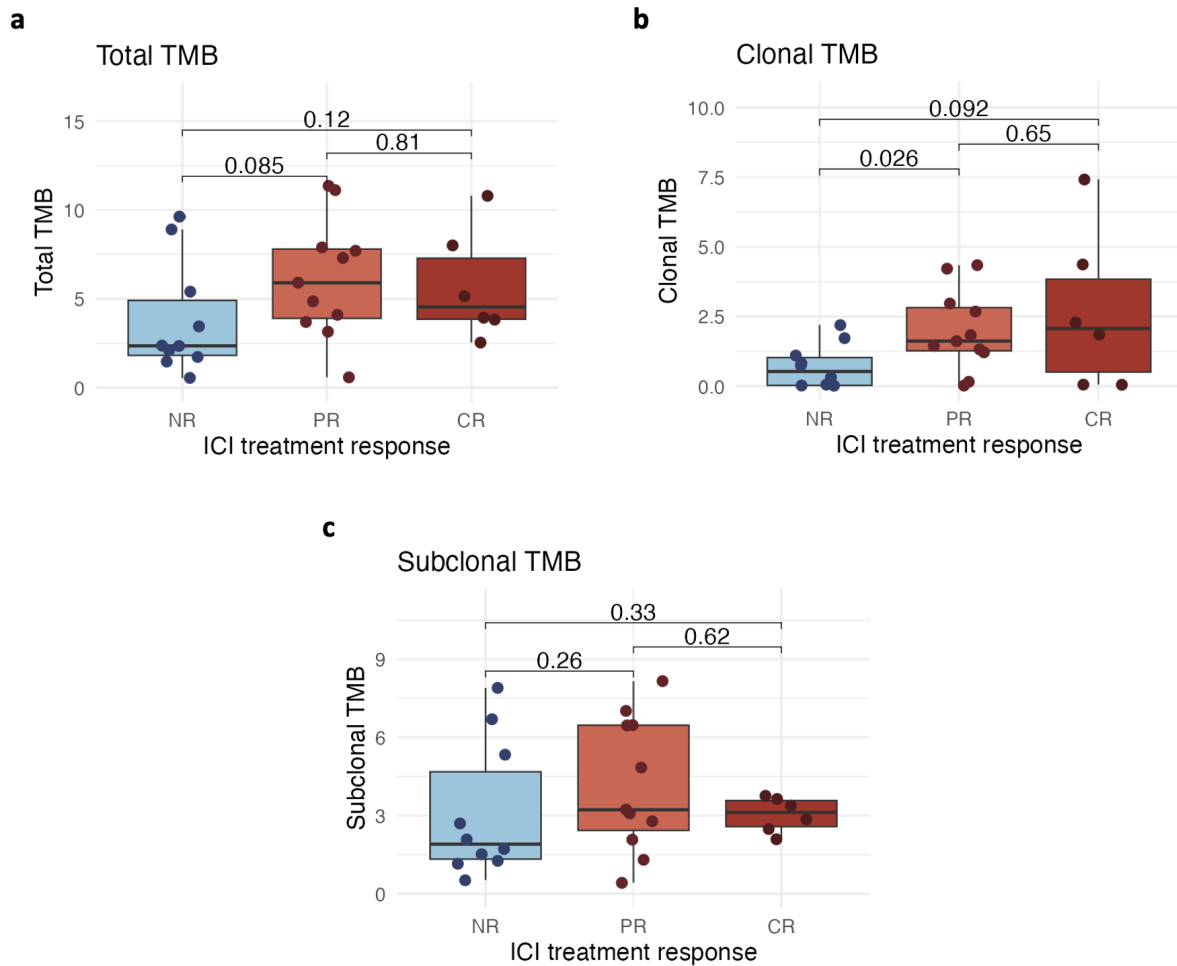
#co-corresponding authors



**Figure S1. Pairwise nucleotide substitution patterns in the urothelial cancer cohort of the Cancer Genome Atlas (TCGA).** The frequency of transitions (Ti) and transversions (Tv) is also shown. The number of samples is 411.

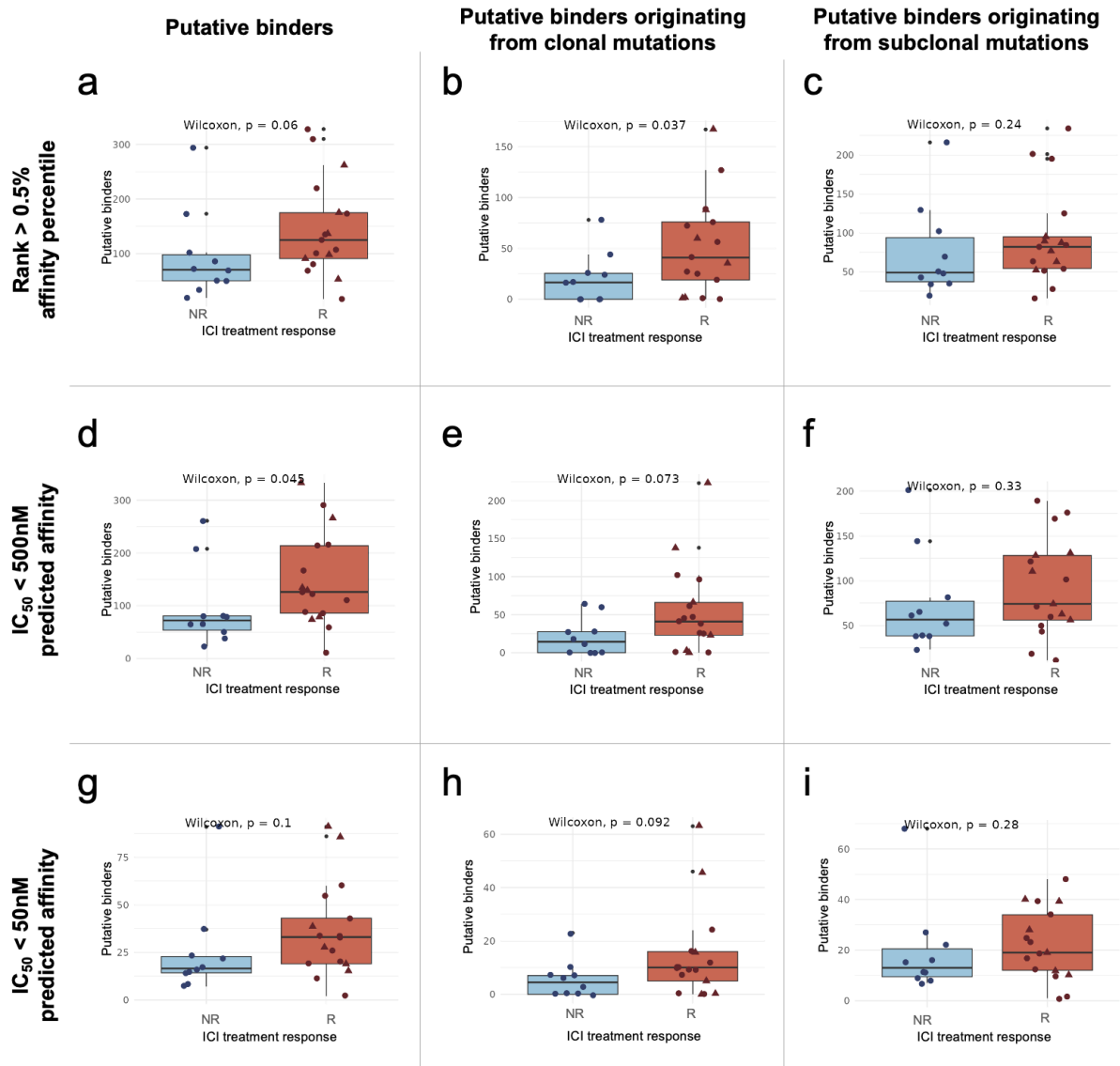


**Figure S2. Relationship between APOBEC mutations and response to treatment. a. APOBEC enrichment in clonal mutations.** There is a significant positive relationship between response to treatment and the APOBEC enrichment in clonal mutations ( $p$ -value = 0.03, Wilcoxon rank sum test). **b. APOBEC enrichment in all mutations.** The differences between responders and non-responders are not statistically significant. NR: no responders, R: responders, triangle shape represents the complete responders among the responder group.



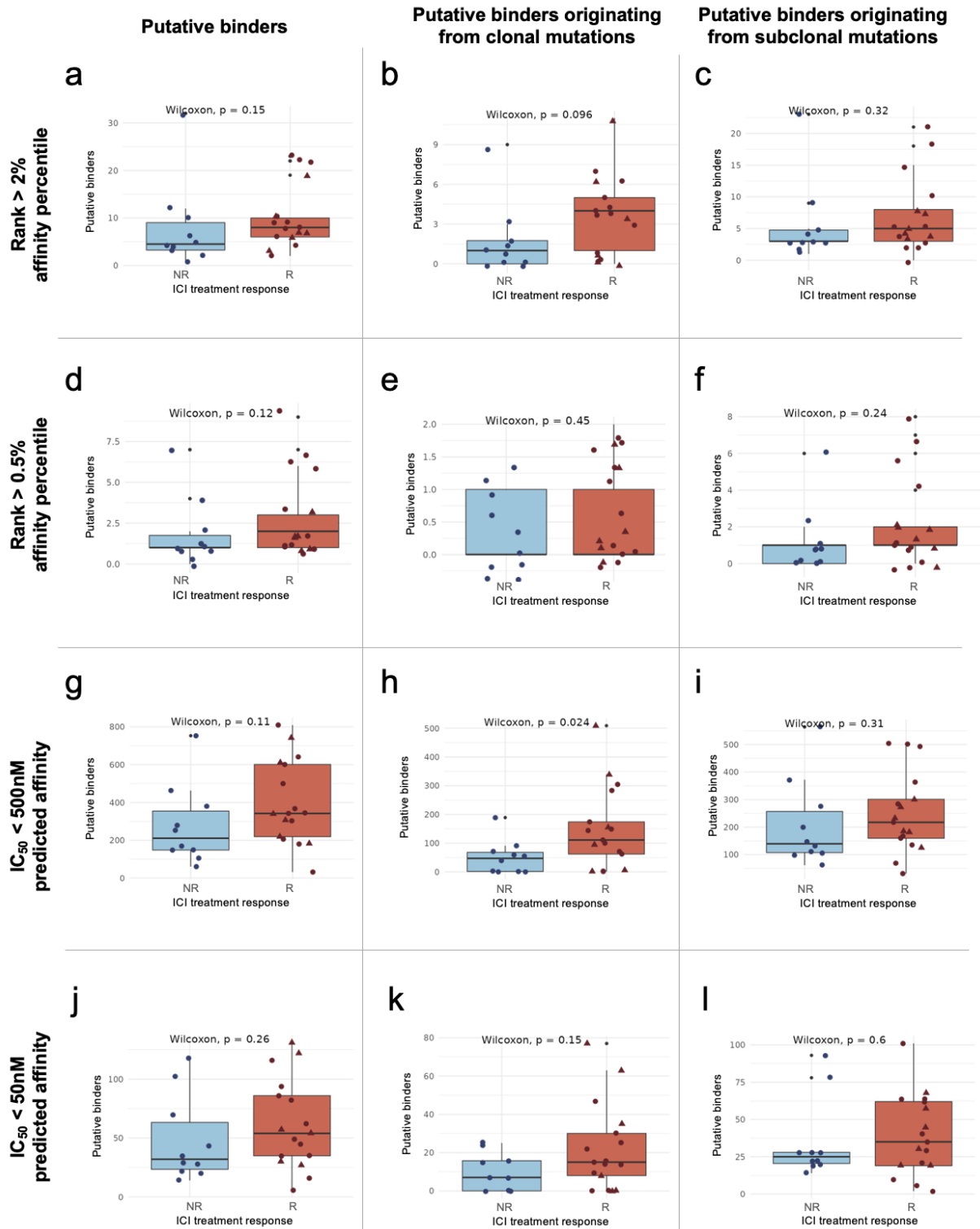
**Figure S3. Relationship between TMB and the three different response groups to ICI therapy. a. Relationship between TMB and response to ICI treatment.** The differences in TMB values between the three response groups were not significant. **b. Relationship between clonal TMB and response to ICI treatment.** The clonal TMB for partial responders is significantly higher compared to non-responders (p-value = 0.026). The differences in clonal TMB between non-responders and complete responders and partial responders compared to complete responders did not reach statistical significance. **c. Relationship between subclonal TMB and response to ICI treatment.** The differences in subclonal TMB values between the three response groups were not significant. NR: no responders, PR: partial responders, CR: complete responders.

# NetMHCpan 4.0



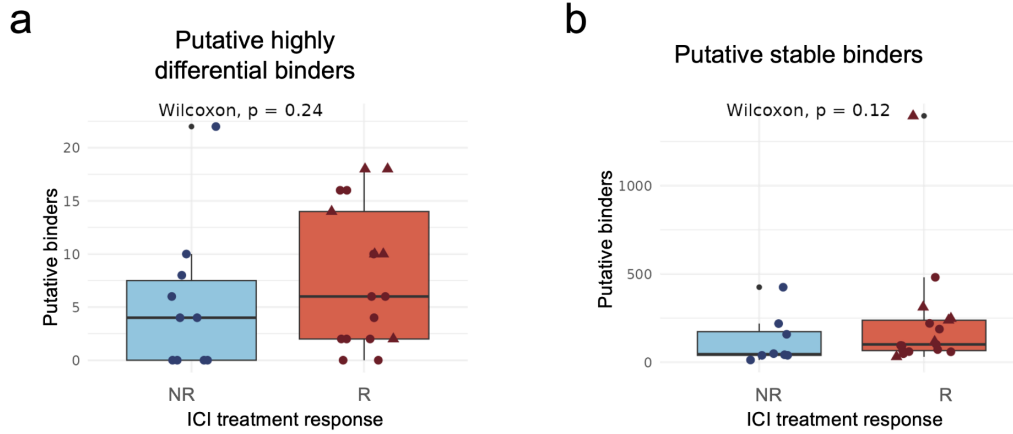
**Figure S4. Relationship between ICI treatment response and the number of putative binders predicted with NetMHCpan 4.0.** The number of predicted binders tends to be higher in responders than in non-responders. **a-c:** Number of putative binders with predicted affinity rank < 0.5%. **d-f:** Number of putative binders with predicted affinity  $IC_{50} < 500nM$ . **g-i:** Number of putative binders with predicted affinity  $IC_{50} < 50nM$ . P-values were calculated using the Wilcoxon rank sum test. NR: no responders, R: responders, triangle shape represents the complete responders among the responder group.

# MHCflurry 2.0



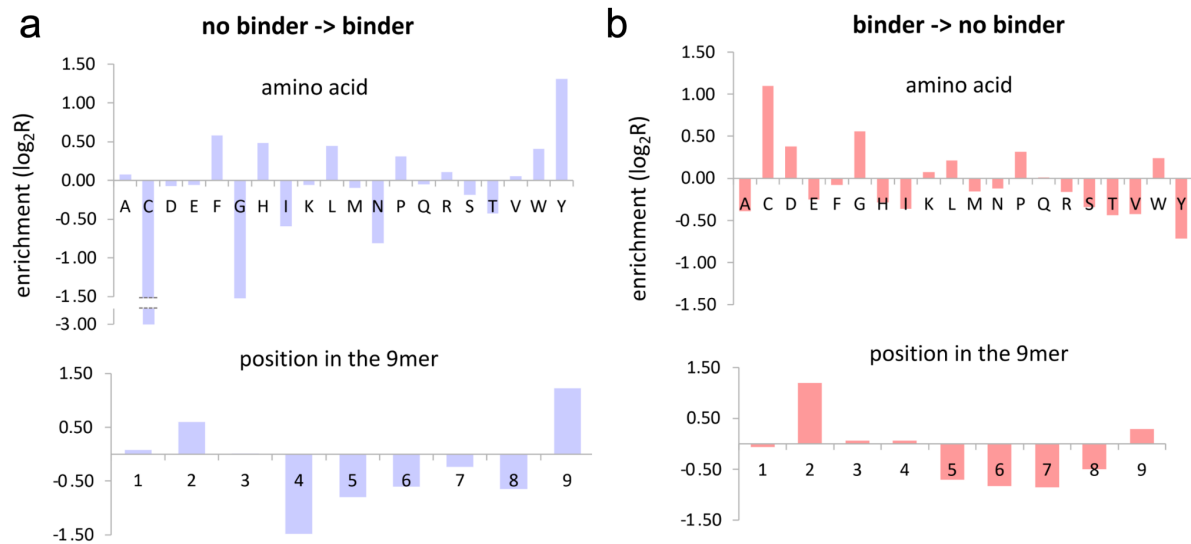
**Figure S5. Relationship between ICI treatment response and the number of putative binders predicted with MHCflurry 2.0.** The number of putative binders tends to be higher in responders than non-responders. **a-c:** Number of putative binders with predicted affinity rank < 2%. **d-f:** Number of putative binders with predicted affinity rank < 0.5%. **g-i:** Number of putative binders with predicted affinity  $IC_{50} < 500nM$ . **j-l:** Number of putative binders with predicted affinity  $IC_{50} < 50nM$ . P-values were

calculated using the Wilcoxon rank sum test. NR: no responders, R: responders, triangle shape represents the complete responders among the responder group.

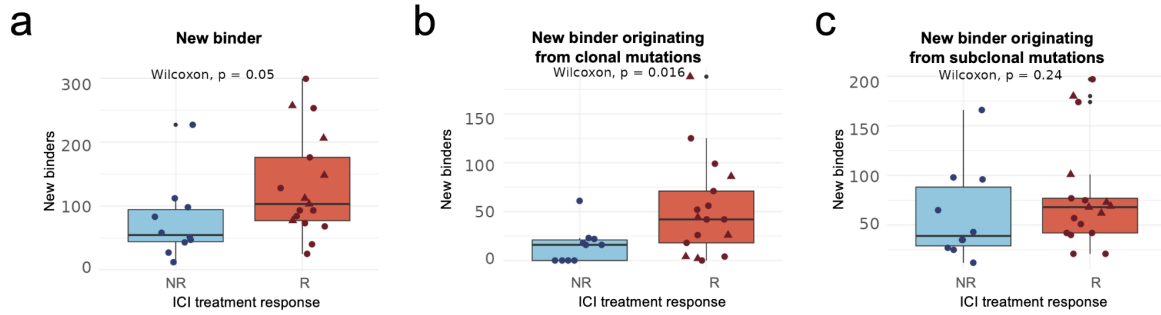


**Figure S6. a. Relationship of differential agretopicity index (DAI) and treatment response.** No significant difference in highly differential peptides ( $DAI > 9$ ) was seen between response groups. **b. Relationship between the number of predicted stable binders and treatment response.** No significant difference in the number of putative stable binders (binding stability  $< 1.4h$ ) was seen between response groups. P-values were calculated using Wilcoxon rank sum test. NR: no responders, R: responders, triangle shape represents the complete responders among the responder group.

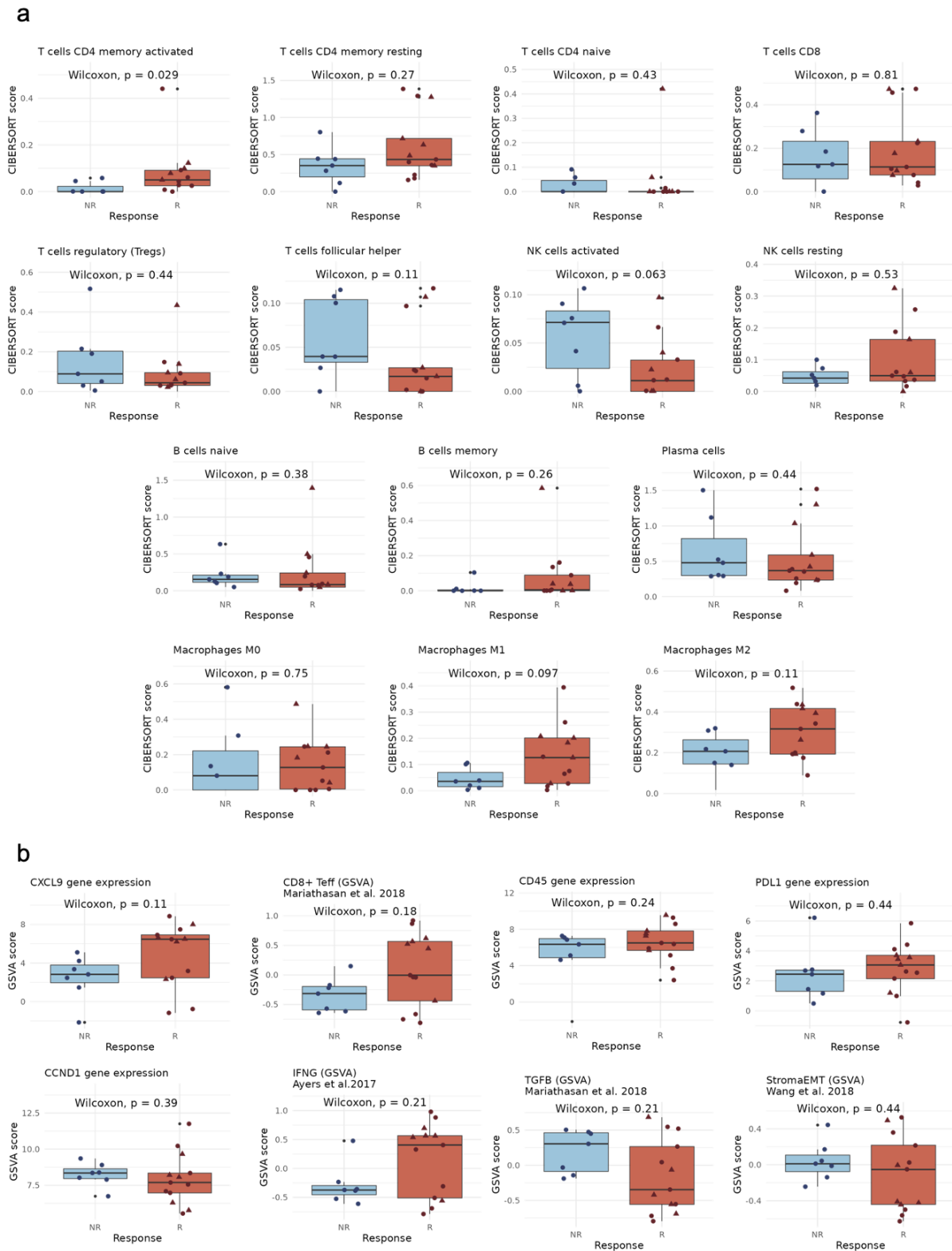




**Figure S7. Non-synonymous mutations affect the binding affinity of the peptide. a. Formation of new MHC I binders.** Enrichment for different amino acid substitutions (above) or positions in the peptide (below) are measured as the log<sub>2</sub> ratio of the substitution frequency in the set of new binders versus the frequency in the set of peptides that do not change binding status. Enriched amino acids using a chi-square test: tyrosine (Y), phenylalanine (F), leucine (L) and histidine (H) at p-value < 10<sup>-5</sup>, tryptophan (W) at p-value = 0.002872. **b. Loss of MHC I binding capacity.** Enrichment for different amino acid substitutions (above) or positions in the peptide (below) are measured as the log<sub>2</sub> ratio of the substitution frequency in the set of peptides associated with loss of MHC I binding *versus* the frequency in the set of peptides that do not change their binding status. Enriched amino acids using a chi-square test: cysteine (C) (p-value < 10<sup>-5</sup>), glycine (G) (p-value = 6.55x10<sup>-5</sup>).

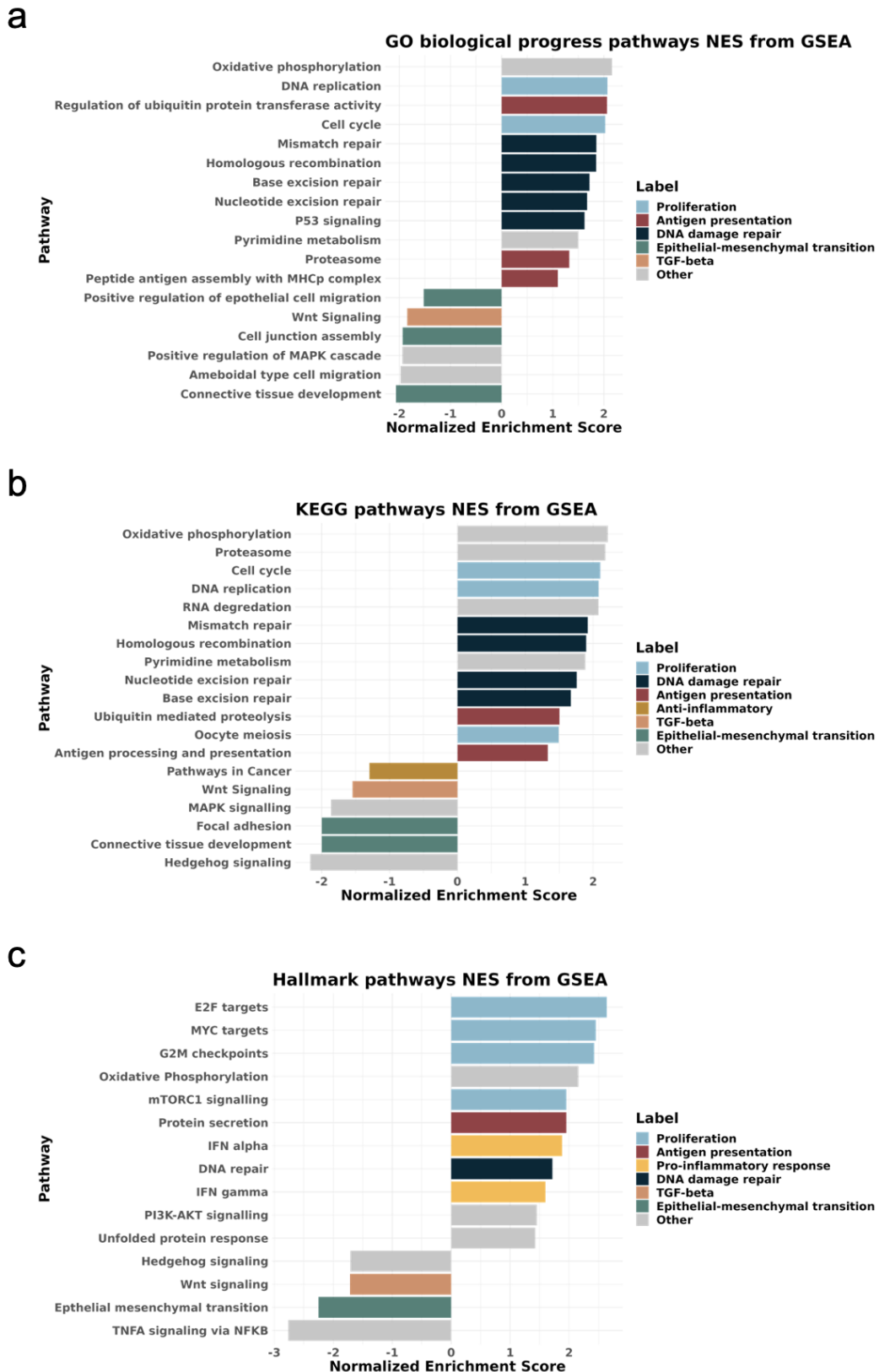


**Figure S8. Relationship of number of predicted new binders and treatment response. a. Binders derived from total mutations.** Responders have a higher number of new putative binders than non-responders (Wilcoxon test,  $p$ -value = 0.05). **b. Binders derived from clonal mutations.** Number of putative binders originating from clonal mutations is significantly higher in responders than non-responders (Wilcoxon test,  $p$ -value = 0.016). **c. Binders derived from subclonal mutations.** No significant difference can be observed for the number of putative binders originating from subclonal mutations between responders and non-responders. NR: no responders, R: responders, triangle shape represents the complete responders among the responder group.

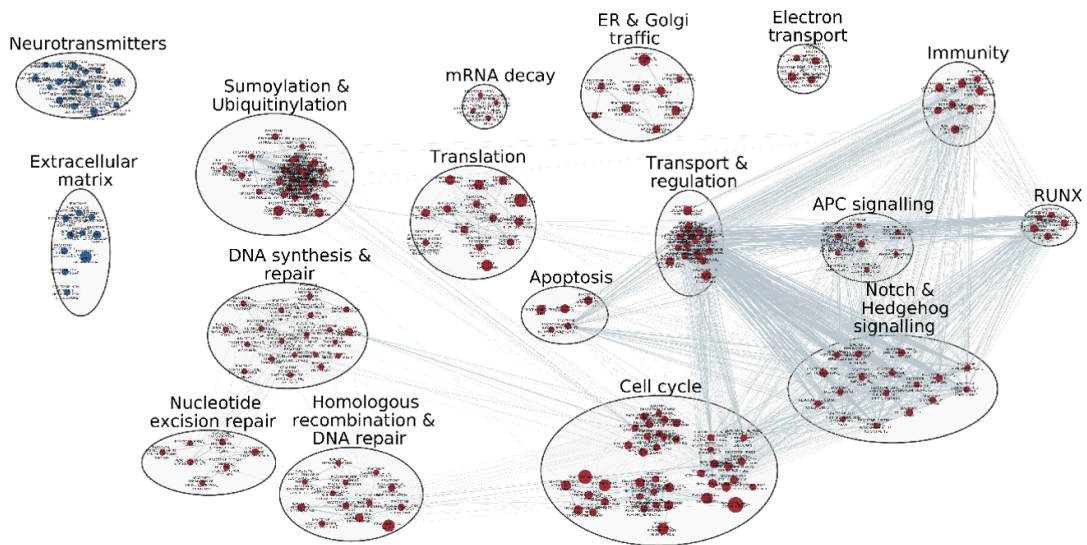
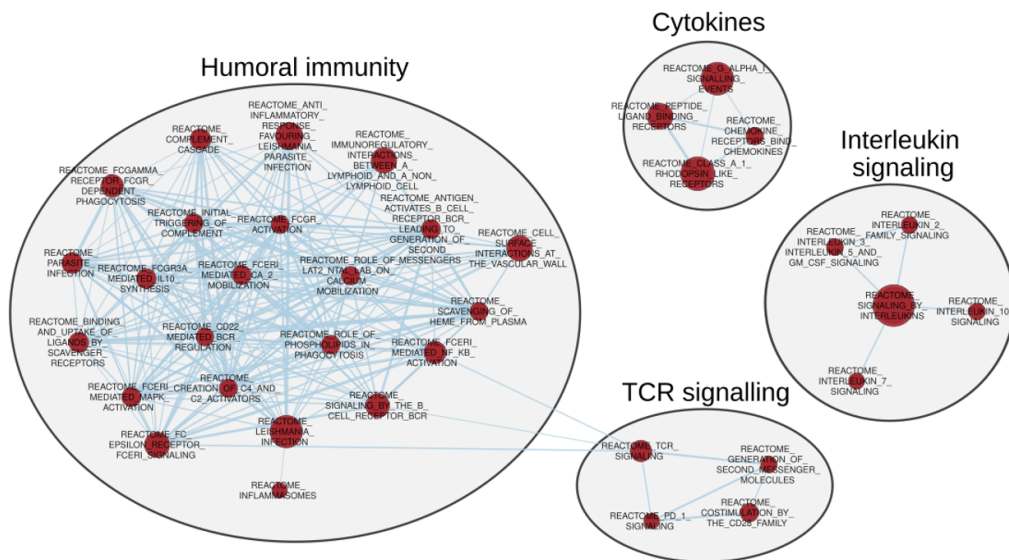


**Figure S9. Relation between tumor-infiltrating estimated immune cells abundances and immune biomarkers and treatment response.** Boxplots comparing **a. abundance** of immune cells and treatment response and **b. expression** of different immune-related genes (log2CPM) and signatures (GSVA scores). Immune cell infiltration was estimated with CIBERSORT using gene

expression profiles. P-values were calculated using Wilcoxon rank sum test. Details on immune biomarkers and immune cell profiles can be found in the supplementary data file 2. NR: no responders, R: responders triangle shape represents the complete responders among the responder group.



**Figure S10. Pathways of gene set enrichment analysis significantly related to ICI response** (adjusted  $P < 0.05$ , comparing 13 responders and 7 non-responders). Selected pathways are shown. The complete list of pathways with their adjusted p-value, normalized enrichment score and the included genes is provided in the Additional data file 3.

**a****b**

**Figure S11. Network of significantly enriched pathways.** Enrichment map of GSEA results (adjusted  $p$ -value  $< 0.05$ ) comparing **a.** responders *versus* non-responders and **b.** complete responders *versus* partial-responders. Nodes represent genesets and edges represent the connectivity between genesets (combined metric Jaccard+Overlap  $> 0.375$ ). Red and blue represent positive and negative enrichment scores, respectively.

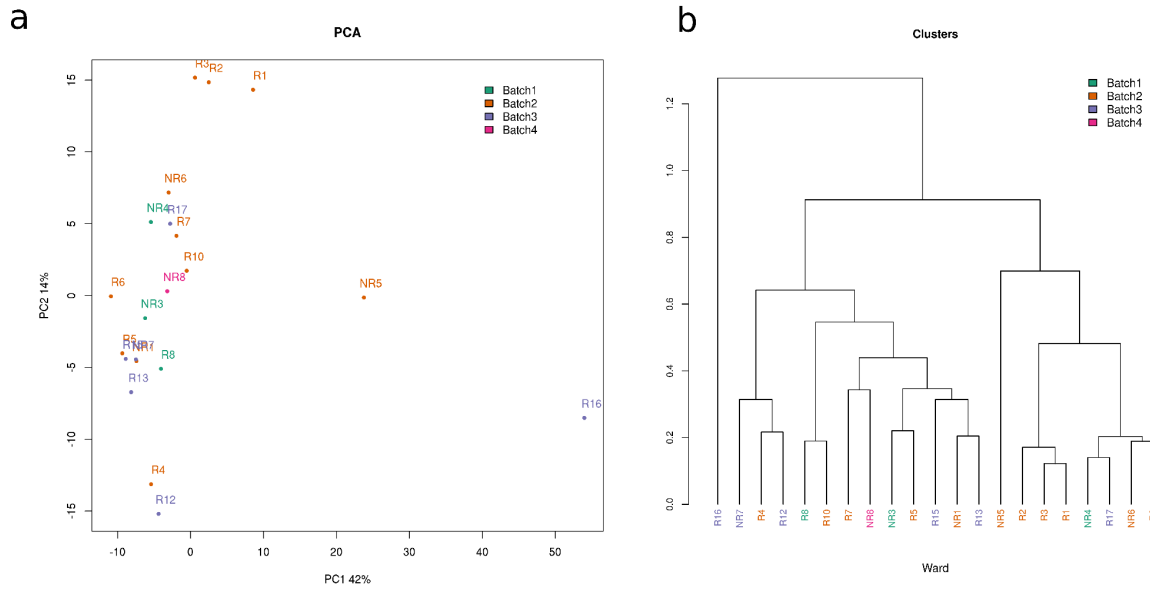


**Figure S12. Quality control of RNASeq data. a.** PCA using the top 500 most variable genes. **b.** Dendrogram using the top 500 most variable genes, 1-correlation distance and Ward2 linkage method. R16 was detected as an outlier. No batch effect was present.

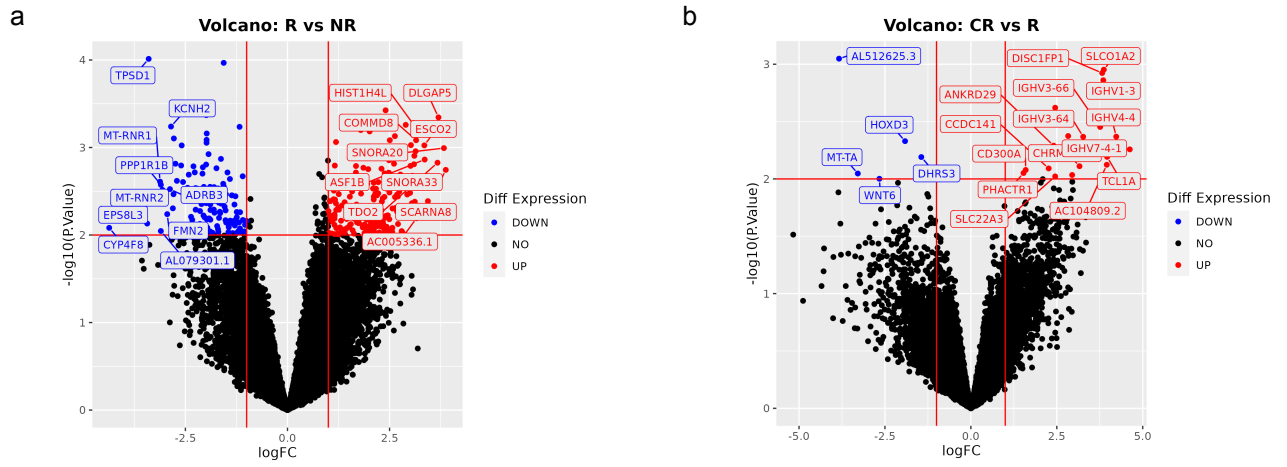


**Figure S13. Differentially expressed genes.** Volcano plots showing the results of the contrasts: **a.** responders vs non-responders. **b.** complete responders vs partial responders. The thresholds used in the plots are  $P.Value < 0.01$  and  $|\logFC| > 1$